ELSEVIER

Chemical Geology 126 (1995) 1–16

CHEMICAL GEOLOGY
INCLUDING
ISOTOPE GEOSCIENCE

Generation of plume magmas through time: an experimental perspective

Claude Herzberg

Department of Geological Sciences, Rutgers University, New Brunswick, NJ 08903, USA
Center for High Pressure Research and Mineral Physics Institute, The State University of New York at Stony Brook, Stony Brook, NY 11794, USA

Accepted 11 November 1994; accepted 31 July 1995 after revision

Abstract

Experimental melting studies indicate that secular variations in the geochemistry of many komatiites were determined by secular variations in the depth of melt segregation in plumes. Higher pressures stabilize garnet relative to olivine and pyroxenes, resulting in komatiites with lower Al_2O_3, and higher CaO/Al_2O_3 and Gd/Yb. The experimental work is consistent with the following pressures of melt segregation: 3–4 GPa for Tertiary and Cretaceous picrites and komatiites; 5–7 GPa for most komatiites with 2.7-Ga ages; and 9–14 GPa for komatiites with 3.5-Ga ages. Melting and melt segregation occurred deeper in the past largely because the Earth was hotter, and komatiites are a thermometer of this secular cooling. Depth of melting is critically dependent on internal plume temperature, and the geochemistry of most komatiites can be explained by plumes that were ~200°C hotter than the secular cooling Earth model of F.M. Richter. Hot Archean plumes that were 300–400°C above ambient mantle could have experienced melting in the transition zone and the top of the lower mantle. Geological evidence in support of hot plumes is rare, but the best examples can be found in the 2.7-Ga komatiites from the Boston Township of Ontario and the 3.3-Ga peridotite xenoliths from the Kaapvaal craton.

1. Introduction

There is a growing consensus that komatiites formed in plumes rather than along spreading ridges (Fyfe, 1978; Jarvis and Campbell, 1983; Arndt, 1986; Campbell et al., 1989; Miller et al., 1991; Storey et al., 1991; Herzberg, 1992; Nisbet et al., 1993; Xie et al., 1993; Abbott et al., 1994). Important questions involve the thermal characteristics of these plumes compared to ambient mantle, the depth of melting, the relationship between komatiites and basalts, and how these factors changed through time. High-pressure phase equilibrium studies are beginning to provide answers to these questions because it is becoming evident that there occurs considerable changes in the major-element geochemistry of liquids as a function of temperature and pressure (Herzberg, 1992). Komatiites therefore provide a record of the temperatures and pressures of melting and melt segregation.

This contribution is a progress report of experimental work on the anhydrous phase equilibrium relations of komatiite and peridotite that I have personally been involved in at the Stony Brook High Pressure Laboratory (Herzberg et al., 1990; Herzberg, 1992, 1993a, b; Zhang and Herzberg, 1994a, b; Herzberg and Zhang, 1995). These studies have stressed the importance of evaluating the compositions of high-pressure liquids at all points in the melting interval, from small melt fractions on the solidus to large melt fractions near the liquidus.

SSDI 0009-2541(95)00099-2

The compositions of liquids on the solidus are difficult to determine experimentally at any pressure (Herzberg, 1992; Hirose and Kushiro, 1993; Baker and Stolper, 1994) in part because of difficulties in segregating small melt fractions from a peridotite source, and also because the liquids can be modified by quench crystallization at the termination of an experiment. Many of these difficulties have been avoided by adoption of the "shotgun" experimental method (O'Hara, 1968) wherein liquid compositions on the solidus [L + Ol + Opx + Cpx + Gt] have been bracketed by examining the nature of the liquidus phase for a wide range of komatiite compositions. The drawback is that the shotgun method is labor-intensive and it is somewhat impractical for determining the concentrations of incompatible elements such as Na_2O at very low melt fractions. But because most komatiites were formed by melting in the 25–50% range, their Na_2O contents are low ($\sim$0.5%). Indeed 98–99% of the geochemistry of most komatiites can be represented in the system CaO–MgO–FeO–Al_2O_3–SiO_2 (Herzberg, 1992), and the shotgun method is ideally suited for understanding komatiites in simplified analogue systems. The liquids on the solidus reported here are based on experimental data in the systems CaO–MgO–FeO–Al_2O_3–SiO_2 (Bertka and Holloway, 1988) and CaO–MgO–Al_2O_3–SiO_2 (Davis and Schairer, 1965; Presnall et al., 1979; Fujii et al., 1989; Herzberg, 1992); these data have been parameterized as a function of pressure, the composition of olivine in the source region and the degree of partial melting (Herzberg, 1992). For liquids in the 2.3–10-GPa range, this technique has resulted in calculated and observed liquid compositions that differ by no more the following relative amounts: $\pm$5% for SiO_2, Al_2O_3 and MgO; and $\pm$8% for FeO and CaO (Herzberg, 1992). Experiments completed at 5 GPa in the system CaO–MgO–FeO–Fe^0–Al_2O_3–SiO_2 (Herzberg, 1993b) yielded a liquid composition that is well within the error of the parameterized 5-GPa solidus liquid. Solidus liquids in the 10–14-GPa range are extrapolated from these parameterizations, and those in the 14–18-GPa range are based on electron microprobe work on experiments formed on peridotite KLB-1 (Herzberg et al., 1990; Herzberg and Zhang, 1995). Although much more experimental work needs to be done, the data that are currently available are permitting the first quantitative estimates of depths of melting of komatiites.

Experimental data have also been reported for naturally-occurring komatiites (Wei et al., 1990; Tronnes et al., 1992), but because the distinction between clinopyroxene and orthopyroxene was not made, these results cannot be used to constrain the CaO/Al_2O_3 for liquids on the solidus, a parameter that is emphasized throughout this paper. Experiments have also been done on komatiite analogue compositions for the purpose of evaluating the partitioning behavior of trace elements between garnet and liquid (Kato et al., 1988; Ohtani et al., 1989; Yurimoto and Ohtani, 1992), but again the results do not provide information on the major-element composition of liquids on the solidus. This paper also does not include some new but unpublished data on the melting of peridotite KLB-1 from Japan (Shimazaki and Takahashi, 1993; E. Takahashi, pers. commun., 1994), but readers should note that there is now a great deal of consistency in the *T–P* phase diagram emerging from Tokyo and the one published by us (Fig. 1; Zhang and Herzberg, 1994a).

2. The MgO content of liquids in the melting interval

The experimental data that have been acquired to 20-GPa range demonstrate that the effect of pressure is to increase the MgO content of liquids generated on the anhydrous solidus, and basalts transform to picrites and komatiites (O'Hara, 1968; O'Hara et al., 1975; Herzberg and O'Hara, 1985; Falloon and Green, 1988; Herzberg, 1992; Langmuir et al., 1992). This is shown in Fig. 1 together with the latest phase diagram for anhydrous peridotite KLB-1 (Zhang and Herzberg, 1994a). The MgO contents on the solidus are based on the CaO–MgO–FeO–Al_2O_3–SiO_2 parameterization discussed above (Herzberg, 1992), but with MgO adjusted downward in order to facilitate a comparison with basalts that contain $\sim$1% Na_2O. Although high-pressure experimental data involving Na_2O are sparse, the parameterizations of Langmuir et al. (1992) indicate that within the garnet stability field, an increase of 1 wt% Na_2O will decrease MgO content by $\sim$2%. Most komatiites contain $<$0.5% Na_2O, and this low amount results from the dilution effect of fairly large degrees of melting, typically 30–50% (Hanson and Langmuir, 1978; Herzberg, 1992).

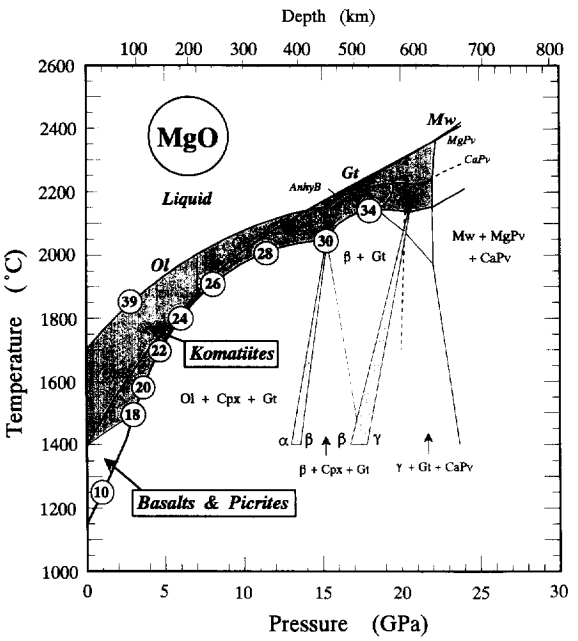

Fig. 1. The MgO content of liquids between the solidus and liquids for a peridotite source with 39% MgO (by weight). *Shaded region* represents komatiite liquids with MgO ≥ 18% and ~1% Na_2O. Basalts and picrites are stable at pressures ≤3–4 GPa; the MgO content at 1 GPa is from Baker and Stolper (1994; ~3% Na_2O). The phase diagram is for anhydrous peridotite KLB-1 (Zhang and Herzberg, 1994a). *Symbols*: *Ol* = olivine; *Opx* = orthopyroxene; *Cpx* = clinopyroxene; *Gt* = garnet; *AnhyB* = anhydrous B; *Mw* = magnesiowüstite; *MgPv* = magnesium silicate perovskite; *CaPv* = calcium silicate perovskite; α = olivine; β = modified spinel $(Mg,Fe)_2SiO_4$; τ = spinel $(Mg,Fe)_2SiO_4$. MgO at 15–18 GPa is too high (Herzberg and Zhang, 1995).

The point behind considering sodium is to facilitate a better understanding of the pressure at which liquids on the solidus transform from basaltic to komatiitic. Komatiites, as defined by liquids with ≥18% MgO that solidified to spinifex-textured rocks (Arndt and Nisbet, 1982), should be stable on the solidus at pressures between 3 and 4 GPa (Fig. 1), depending on Na_2O. This compares favorably with a 3.5-GPa experimental determination of Falloon and Green (1988), who reported a liquid with 19.99% MgO and 1.31% Na_2O for the solidus assemblage [L + Ol + Opx + Cpx + Gt]. The parameterization of Langmuir et al. (1992) indicates that liquids with 18% MgO will be stable on the solidus at 3.0 GPa if Na_2O is 1% and 4.0 GPa if Na_2O is 2%. At 1 atm, a komatiite with 18% MgO and 1% Na_2O will be stable at temperatures that are ≥1400°C (Fig. 1; Beattie, 1993). Throughout most *T–P* conditions of melting in the upper mantle and transition zone, liquids generated by the partial melting of mantle peridotite will be komatiitic. By comparison, basalts and picrites are confined to very low pressures of melting and a *T–P* stability field that is restricted to the bounds shown in Fig. 1.

3. The Al_2O_3 content and CaO/Al_2O_3 of liquids in the melting interval

Pressure stabilizes garnet with respect to pyroxenes and olivine (Herzberg, 1983; Zhang and Herzberg, 1994a, b). This is most obviously illustrated in the phase diagram for mantle peridotite at 14 GPa where the liquidus phase for KLB-1 changes from olivine to garnet (Fig. 1 and Fig. 2). The solubility of garnet in silicate liquids is therefore reduced, and this results in high-pressure magmas that can have very low concentrations of Al_2O_3, comparable to many alumina-depleted komatiites. In Fig. 2, it can be seen that Al_2O_3 drops from 13% at a pressure of 3 GPa to ~4% at 9 GPa. At greater pressures, the content of Al_2O_3 in mag-

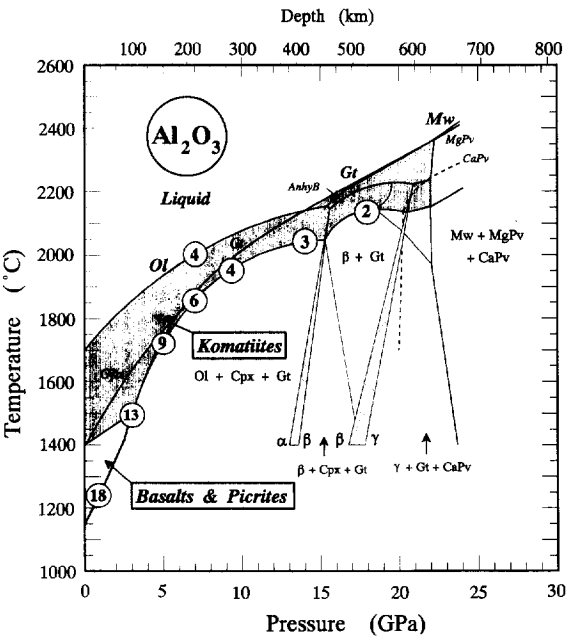

Fig. 2. The Al_2O_3 content of liquids between the solidus and liquidus for a peridotite source with 4% Al_2O_3 (by weight); 1-GPa datum is from Baker and Stolper (1994).

mas on the solidus can be lower than the Al_2O_3 content of fertile mantle peridotite, which is typically 4%. The value shown at 18 GPa is 2%, but this is based on preliminary electron microprobe work on KLB-1 experiments, and it is subject to a probable relative uncertainty of ±50% (Herzberg and Zhang, 1995).

The ratio CaO/Al_2O_3 is strongly dependent on pressure because variations in the CaO content of magmas on the solidus are not as pronounced as those for Al_2O_3 (Herzberg, 1992). For liquids on the solidus [L + Ol + Opx + Cpx + Gt], variations in CaO/Al_2O_3 are shown as the solidus line in Fig. 3a, and they can be retrieved from the empirical equations:

$$CaO\ (wt\%) = 16.0811 - 2.0724P + 0.1322P^2 - 0.0018P^3$$

$$Al_2O_3\ (wt\%) = 22.8581 - 4.0110P + 0.2703P^2 - 0.0061P^3$$

where P is the pressure in GPa. At pressures in the 2.5–6-GPa range where there exists the greatest amount of experimental data, the ratio CaO/Al_2O_3 seems to be insensitive to variations in composition of the source region and the degree of partial melting on the solidus (see fig. 5 in Herzberg, 1992). But there are a number of important factors that can affect it, and these are summarized in Fig. 3a and b.

The parameter CaO/Al_2O_3 is buffered by the solidus assemblage [L + Ol + Opx + Cpx + Gt], and it is the stability of clinopyroxene and garnet that is most important in regulating it. When Cpx or Gt are consumed by increased melting, CaO/Al_2O_3 will be free to change. In the 2.5–4-GPa pressure range, garnet will be the first phase to melt, and the course of increased melting will involve [L + Ol + Opx + Cpx] → [L + Ol + Opx] → [L + Ol] → [L]. The dissolving of Cpx along the cotectic [L + Ol + Opx + Cpx] will result in a liquid with reduced Al_2O_3 and increased CaO/Al_2O_3; these supersolidus liquids will plot to the right of the solidus line in Fig. 3a. After all Cpx is dissolved (i.e. [L + Ol + Opx] and [L + Ol]) the parameter CaO/Al_2O_3 will remain fairly constant and similar to that for the peridotite source being melted, that is the vertical line in Fig. 3a. Mantle peridotite exhibits a range of values for CaO/Al_2O_3 and Al_2O_3, and these are summarized in the Appendix.

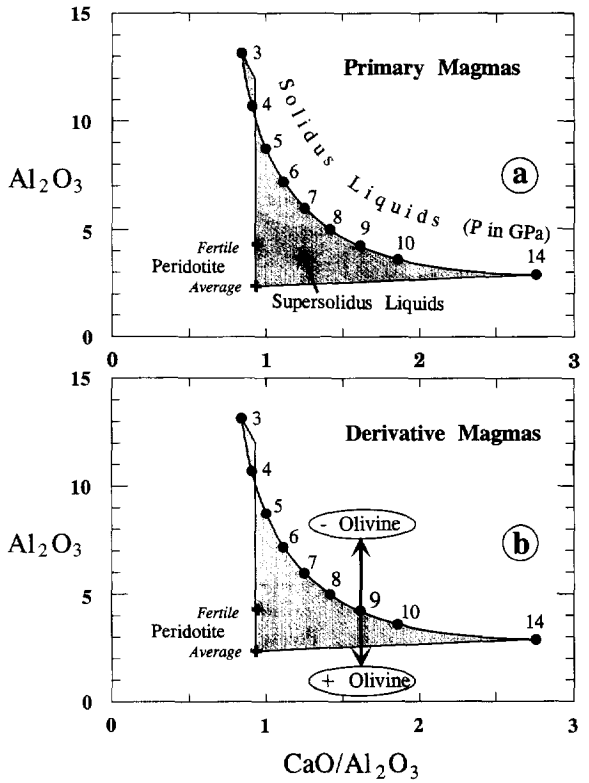

Fig. 3. a. Al_2O_3 (wt%) and CaO/Al_2O_3 (by weight) for primary magmas generated between the solidus and the liquidus (*shaded sail*). Fertile and average mantle peridotite are from Stosch and Seck (1980; Ib8) and Herzberg (1993a), respectively. *Numbers* refer to pressures in GPa along the solidus.
b. Al_2O_3 (wt%) and CaO/Al_2O_3 (by weight) for derivative magmas formed by olivine addition and subtraction of primary magmas.

In the 4–9-GPa range, progressive melting will exhaust Cpx first, and involve [L + Ol + Opx + Gt] → [L + Ol + Opx] → [L + Ol] → [L]. The dissolving of Gt along the cotectic [L + Ol + Opx + Gt] will change the liquid by increasing slightly Al_2O_3 and lowering substantially CaO/Al_2O_3; these supersolidus liquids will plot to the left of the solidus line in Fig. 3a. When all Gt is dissolved, CaO/Al_2O_3 for the liquid will remain fairly constant for the assemblages [L + Ol + Opx], [L + Ol] and [L], similar to the source. At pressures greater than ~9 GPa, advanced melting will involve [L + Ol + Gt] because orthopyroxene is no longer a crystallizing phase (Fig. 1 and Fig. 2), and the melting of garnet will continue to reduce CaO/Al_2O_3 in the liquid. Liquids will reflect CaO/Al_2O_3 of the source when garnet is totally melted

(i.e. [L + Ol]), or when melting is total. Primary magmas that are generated on the solidus, at supersolidus conditions, and on the liquidus will adopt the contents of Al_2O_3 and CaO/Al_2O_3 that are shown by the "sail" in Fig. 3a.

The abundance of olivine cumulates in komatiite flows demonstrates that primary komatiite magmas are never preserved, and even spinifex-textured rocks may be cumulates (Nisbet et al., 1993). But because olivine contains such small amounts of CaO and Al_2O_3, these derivative magmas will maintain the same CaO/Al_2O_3 as the primary magmas. A komatiite flow that has had olivine added will have a lower value for Al_2O_3, and residual liquids that have had olivine removed will have higher Al_2O_3. These effects are shown in Fig. 3b.

4. The Al_2O_3 content and CaO/Al_2O_3 of plume basalts, picrites and komatiites through time

4.1. Quaternary basalts from Hawaii

Hawaii is a modern plume for which there is the greatest abundance of whole-rock data (e.g., Murata and Richter, 1966; Wright, 1972), and values for Al_2O_3 and CaO/Al_2O_3 contained in tholeiites and alkali basalts are shown in Fig. 4a. The experimentally parameterized values given in Fig. 3a have been extended to 1 GPa with the experimental data of Baker and Stolper (1994) and 2 GPa with the data of Hirose and Kushiro (1993) for KLB-1. Most Hawaiian tholeiites and alkali basalts are from Kilauea, and they cluster at ~13% Al_2O_3 and ~0.75 for CaO/Al_2O_3. This cluster is similar to solidus liquids between 2 and 3 GPa, consistent with the suggestion of Albarède (1992) that most primary magmas from Kilauea segregated at 2–3 GPa. However, most actually plot somewhat to the left of the solidus line. Since primary magmas can only plot on or to the right of this line, it can be inferred that none of the Hawaiian basalts are primary magmas.

The most obvious way to reduce CaO/Al_2O_3 to the left of the line is by fractionation of clinopyroxene (Fig. 4a), although it is possible to explain it by a source region that was inherently low in CaO/Al_2O_3 (see Appendix). Feigenson et al. (1983) modelled clinopyroxene fractionation for the Hawaiian lavas by using the reconstructed aluminous clinopyroxene composition 68 SAL-7 of Beeson and Jackson (1970). This

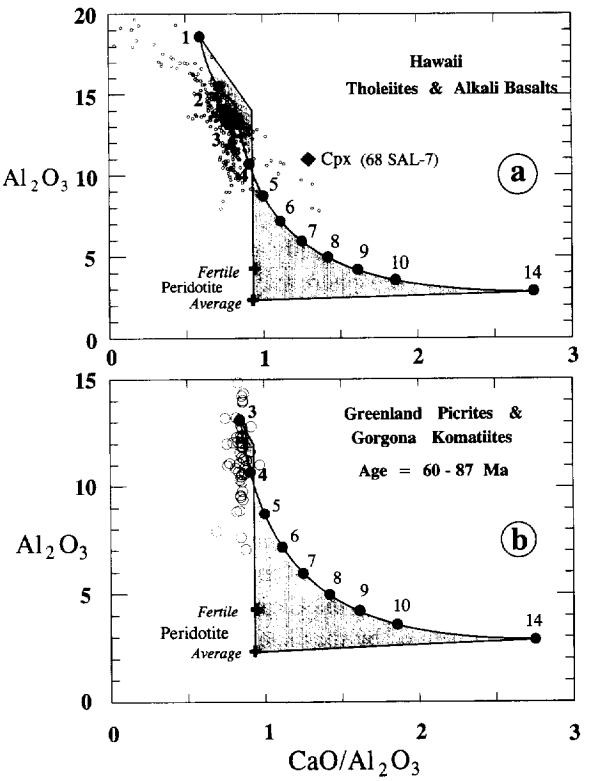

Fig. 4. Al_2O_3 (wt%) and CaO/Al_2O_3 (by weight) for: (a) Hawaiian basalts; and (b) picrites and komatiites from Greenland and Gorgona Island. The *sail* is from Fig. 3a, and *numbers* 1–14 represent the pressures along the solidus in GPa. Rock compositions have FeO = Fe total, and are normalized to 100% anhydrous.

is an appropriate pyroxene composition to use because pyroxene geobarometry has demonstrated that it is of a high-pressure origin (Herzberg, 1978; 2–3 GPa). Removal of this clinopyroxene would be very successful in explaining many of the more evolved alkali basalts that radiate to higher Al_2O_3 and lower CaO/Al_2O_3. The Hawaiian tholeiites and picrites with $Al_2O_3 < 13\%$ are related by olivine addition and subtraction (Feigenson et al., 1983; Albarède, 1992), but even the most primitive of these plot to the low-CaO/Al_2O_3 side of the solidus line. Clinopyroxene removal is again implied, possibly involving fractionation with olivine along the cotectic [L + Ol + Cpx] (e.g., Feigenson et al., 1983). Clague et al. (1991) reported 15% MgO in Hawaiian picritic glasses and recommended a primary magma with 17% MgO; more recent estimates for the primary Kilauean primary magma

contain 16.8% MgO (Hirschmann and Ghiorso, 1994) and 19.2% MgO (Albarède, 1992).

The importance of olivine fractionation has been emphasized repeatedly (e.g., Murata and Richter, 1966; O'Hara, 1968; Wright, 1972; Irvine, 1979; Albarède, 1992; Hirschmann and Ghiorso, 1994), and may be the mechanism by which primary Hawaiian komatiites have been substantially modified. Below it is suggested that the lithosphere may have some influence on whether komatiites erupt or fractionate to basalts.

4.2. *Cretaceous and Tertiary komatiites and picrites from Gorgona Island and West Greenland*

The komatiites from Gorgona Island, which are Cretaceous in age (Kerr and Marriner, 1994), are thought to have been a part of the Caribbean Plateau (Storey et al., 1991) formed by the Galápagos hot spot (Duncan and Hargraves, 1984). Picrites of Tertiary age are found in West Greenland (Holm et al., 1993) and East Greenland (Fitton and Saunders, 1994), and are thought to have formed from the Icelandic plume that accompanied continental breakup. The West Greenland picrites are similar to the Gorgona komatiites (Echeverria, 1982; Aitken and Echeverria, 1984) except that they are devoid of spinifex textures. West Greenland picrites with MgO contents in the 20–30% range have been reported (Holm et al., 1993), but these are likely to be olivine cumulates.

The Gorgona komatiites and the Greenland picrites are essentially indistinguishable from each other when plotted in Fig. 4b. The essential observation is that they cluster close to the solidus line between 3 and 4 GPa, but there is a definite trend in Al_2O_3 from 7% to 15% at nearly constant CaO/Al_2O_3 (0.85). The most simple interpretation is that the picrites and komatiites were generated at 3–4 GPa, and that the spectrum of Al_2O_3 contents is an artifact of variable amounts of olivine addition and subtraction. The degree of melting estimated for the Gorgona komatiites was likely to have been $<30\%$ (Herzberg, 1992). Unlike Hawaii, there appear to have been no lithospheric effects which have contributed to the fractionation of clinopyroxene, indicating that these magmas erupted directly from the axis of the plume.

4.3. *Archean komatiites of 2.7-Ga age*

The most common type of komatiite which is found in all cratons of 2.7-Ga age is the Munro-type, a term that is used here to refer to their alumina-undepleted character (Nesbitt et al., 1979; Jahn et al., 1982; Gruau et al., 1990). Some of the earliest detailed descriptions were reported by Arndt et al. (1977) for komatiites in the Munro Township of the Abitibi greenstone belt in Canada, but Munro-type komatiites from the Belingwe greenstone belt in Zimbabwe are particularly noteworthy because of their relatively unaltered state (Nisbet et al., 1987).

The Munro-type komatiite data base shown in Fig. 5a is from the compilation in Herzberg (1992; references cited therein), and it reveals some of the

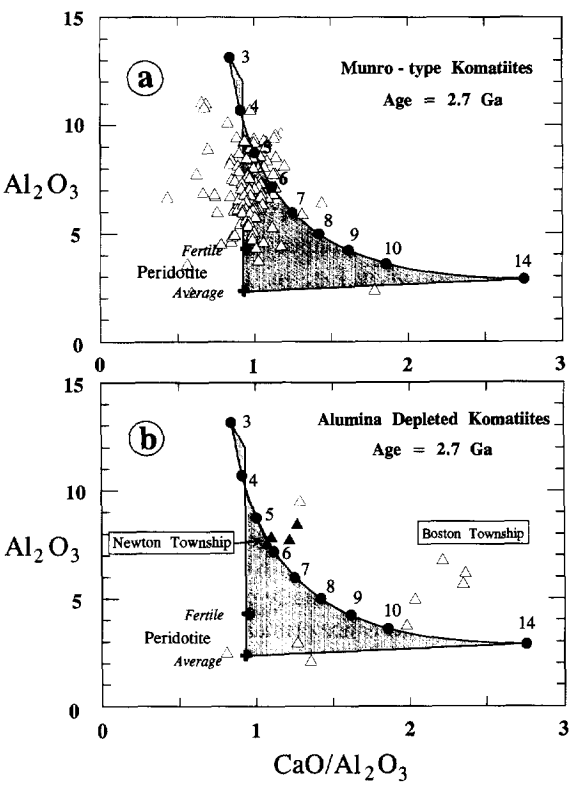

Fig. 5. Al_2O_3 (wt%) and CaO/Al_2O_3 (by weight) for: (a) Munro-type komatiites from all cratons; and (b) komatiites from the Newton (*closed triangles*) and Boston Townships (*open triangles*) in Canada. The *sail* is from Fig. 3a, and the *numbers* 3–14 represent the pressures along the solidus in GPa. Rock compositions have FeO = Fe total, and are normalized to 100% anhydrous.

more essential geochemical characteristics. The alumina-undepleted character refers to contents of Al_2O_3 that actually range from ~5% to 10%, and the ratio CaO/Al_2O_3 is essentially identical to average mantle peridotite (0.93). Some of these komatiites have Al_2O_3 and CaO/Al_2O_3 that are characteristic of solidus liquids at 5 GPa, but inspection of Fig. 5a shows that these are in the minority. Most Munro-type komatiites could not have been liquids which formed on the solidus because they plot well to the left of the CaO/Al_2O_3 solidus line in Fig. 5a. Instead, they were most likely supersolidus liquids which last equilibrated with a harzburgite residue [L + Ol + Opx] (Herzberg, 1992). Liquids in equilibrium with harzburgite will adopt a mantle-like Gd/Yb (i.e. 1.0) and CaO/Al_2O_3 (Gruau et al., 1990; Herzberg, 1992). The ratio CaO/Al_2O_3 can also be lower than the solidus line because of alteration (see below), but CaO mobility is unlikely to modify the rare-earth elements (REE) which are incompatible with garnet in the residue (Arth et al., 1977; Jahn et al., 1980). Munro-type komatiites also have contents of SiO_2 that vary from ~45% to ~50%, and this is characteristic of the dissolution of orthopyroxene that occurs during advanced melting (Herzberg, 1992). Although it is not obvious in Fig. 5a, some of the variability in Al_2O_3 shown in Fig. 5a is also due to variable amounts of olivine fractionation (Herzberg, 1992, fig. 11 therein). It has been estimated that most of these komatiites formed by 30–40% partial melting of average mantle peridotite (Herzberg, 1992).

There is a small but important minority of komatiites of 2.7-Ga age that have geochemical affinities with the older 3.5-Ga alumina-depleted komatiites, and these are from the Newton Township (Cattell and Arndt, 1987) and the Boston Township (Stone et al., 1987; Xie et al., 1993; McCuaig et al., 1994) of Ontario in Canada. These komatiites are characteristically higher in CaO/Al_2O_3 and Gd/Yb, and lower in Al_2O_3 than most Munro-type komatiites, and Fig. 5b illustrates some of these properties. Komatiites from the Newton Township plot on and above the solidus line, and these can be most easily interpreted as being 6–7-GPa solidus liquids which had experienced some olivine removal. The Boston Township komatiites are even more unusual in being very iron-rich (15–20% FeO; Stone et al., 1987; Xie et al.. 1993) and having some of the lowest Al_2O_3 contents ever reported for a 2.7-Ga komatiite (Fig. 5a and b). Most of the Boston Township komatiites have Al_2O_3 and CaO/Al_2O_3 that plot above the solidus line in Fig. 5b. These can be interpreted as 7–12-GPa solidus liquids, and fractionation of olivine will increase Al_2O_3 to a certain extent, so that they plot above the solidus line. But there is a very high degree of scatter to the plots, indicating the probable involvement of second-stage alteration. The most MgO-rich Boston Township komatiites with the largest amount of cumulus olivine also have the lowest CaO/Al_2O_3, an observation that is common to the older Barberton komatiites (Smith and Erlank, 1982; Herzberg, 1992; Lécuyer et al., 1994). Herzberg (1992) and Lécuyer et al. (1994) interpreted these lower CaO/Al_2O_3 Barberton data as resulting from CaO removal during metamorphic recrystallization, of which the more MgO-rich samples are the most easily altered, and the same may apply to the Boston Township komatiites. However, it is readily evident from Fig. 5b that a lowering of CaO/Al_2O_3 resulting from alteration will give rise to a pressure estimate that is too low. The Boston Township komatiites appear to have recorded in their geochemistry unusually high pressures of melting for komatiites of their age (i.e. 10–14 GPa). This is consistent with majorite garnet in the residue, as indicated by the unusually high depletions in the heavy REE (HREE) and high-field-strength elements (HFSE) (Xie et al., 1993; McCuaig et al., 1994).

4.4. *Archean komatiites of 3.5-Ga age*

The most extensive 3.5-Ga data base is for komatiites from the Barberton Mountain Land in South Africa, but komatiites from the Pilbara Block in Australia share the same geochemical characteristics (Gruau et al., 1987). The Barberton data base compiled in Herzberg (1992) is used here, and supplemented by recent data reported by Lécuyer et al. (1994). These are plotted in Fig. 6 together with some of the younger komatiites reported above. The aluminum-depleted character is readily apparent and although there is a spread of values for CaO/Al_2O_3, most of them cluster at 1.5–2.0, close to the solidus line at 9–10 GPa. The most simple interpretation is that they were generated as high-pressure solidus-like liquids, and samples that plot below and above the line were liquids that experienced variable amounts of olivine addition and subtraction. Barberton komatiites are also depleted in the HREE, and their high Gd/Yb distinguishes them from younger koma-

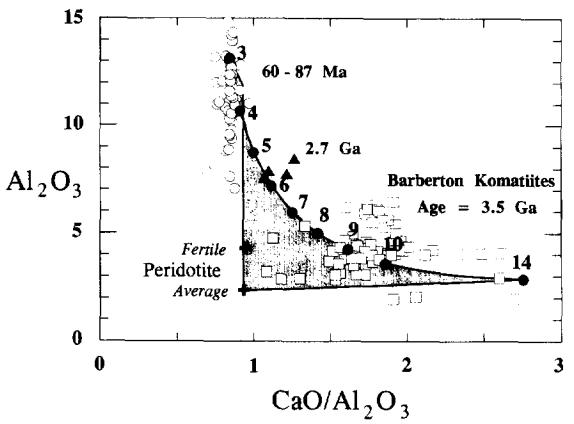

Fig. 6. Al_2O_3 (wt%) and CaO/Al_2O_3 (by weight) for komatiites of all ages. The *sail* is from Fig. 3a, and the *numbers* 3–14 represent the pressures along the solidus in GPa. Rock compositions have FeO = Fe total, and are normalized to 100% anhydrous. *Circles* = picrites from Greenland and komatiites from Gorgona Island (Fig. 4b); *triangles* = Newton Township komatiites (Fig. 5b); *squares* = Barberton komatiites.

tiites (Jahn et al., 1982; Gruau et al., 1990). These essential features, high CaO/Al_2O_3 with high Gd/Yb, have been recognized as a garnet signature since they were first discovered (Nesbitt and Sun, 1976; Sun and Nesbitt, 1978; Nesbitt et al., 1979). These komatiites have the major-and trace-element geochemical characteristics of solidus-like liquids that were last in equilibrium with the assemblage [L + Ol + Gt + Cpx] (Herzberg, 1992), and garnet played a role as a residual phase during the time of melting rather than a cumulate phase during an earlier magma ocean event (Gruau et al., 1990; Herzberg, 1992).

Unlike the younger komatiites, the Barberton samples have a fairly large spread in CaO/Al_2O_3. As discussed above in connection with the Boston Township komatiites, those samples with the lowest CaO/Al_2O_3 are invariably samples with the highest amount of cumulate olivine (Herzberg, 1992; Lécuyer et al., 1994), and are likely to be low because of CaO loss during alteration. If the system was somewhat closed during alteration, it is possible that CaO lost was gained elsewhere, and this could explain Barberton komatiites with ratios of CaO/Al_2O_3 in the 2.0–2.7 range. Alternatively, these high ratios could be an unaltered igneous signature, indicating depths of melt segregation in the 9–14-GPa range.

5. Secular variations in the pressure of melt segregation

There is a very distinctive relationship between the age of komatiite formation and their major-element geochemistry, and this can be tied to the pressure at which these magmas segregated as shown in Fig. 6. Cretaceous age komatiites record a 3–4-GPa signature, most late Archean komatiites of 2.7-GPa age record 5–7 GPa, and early Archean komatiites are the deepest with recorded pressures of 9–14 GPa. This scenario is very similar to the one proposed by Arndt and Lesher (1992) based on the phase equilibrium relations that were available at that time (Takahashi, 1986; Herzberg et al., 1990; Wei et al., 1990) The depth of melting and melt segregation is critically dependent on temperature, and this is examined next.

6. Thermal properties of plumes through time

The pressures recorded by komatiites in Fig. 6 and the phase diagram for mantle peridotite in Fig. 1 can together be used to place constraints on temperatures of melting. An example is shown in Fig. 7 for the generation of the Greenland picrites and the Gorgona komatiites. These magmas have the geochemical properties of liquids formed on the solidus at 3–4 GPa (Fig. 4b), and the *T–P* characteristics of the anhydrous solidus constrain the melting temperature to have been ~ 1600°C (Fig. 1 and Fig. 2). The latent heat of melting will deflect the partially melted adiabat, and an eruption temperature of 1340°C can be inferred from the work of McKenzie and O'Nions (1991, fig. 2 therein).

In the extreme case of instantaneous segregation at the point of melt initiation, melting would be perfectly fractional, and the geochemical record would be that of the initial liquid on the solidus as long as it did not interact with anything else on the way to the surface. If melt segregation did not occur, then no high-pressure geochemical record would exist because the entire melting process would be equilibrium rather than fractional, and the final drops of magma would have a 1-atm geochemistry. The pressure that is recorded in the geochemistry of a komatiite must represent the pressure at which the melt segregated from its matrix, and this will always be at some point between the two extreme

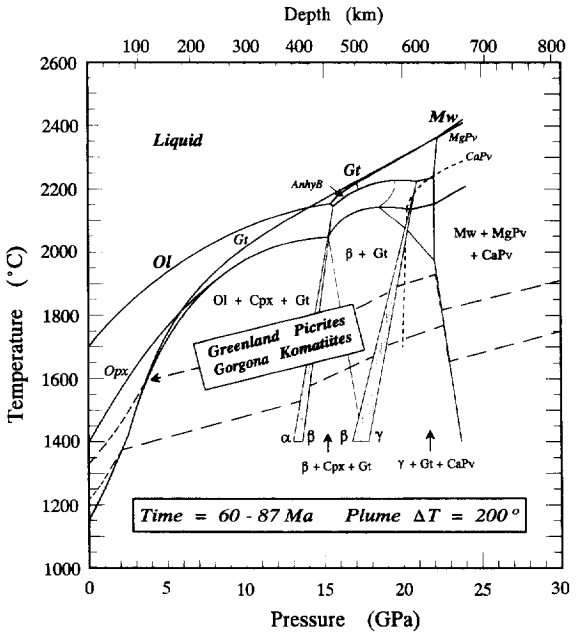

Fig. 7. Formation of the Greenland picrites and Gorgona komatiites. Adiabatic gradients are from two main sources: below the solidus, the adiabats are from Miller et al. (1991), but inflected at the various phase transformations shown (Ita and Stixrude, 1992). Above the solidus, the adiabats are interpolated from those given by McKenzie and O'Nions (1991). A present-day potential temperature of 1350°C is assumed below ridges, elevated somewhat from the 1280°C potential temperature of McKenzie and Bickle (1988) in order for melting to be deep enough to provide a garnet signature in mid-ocean ridge basalts (Salters and Hart, 1989).

possibilities, where equilibrium melting transforms to fractional melting. Any forward model must make explicit assumptions about the physics and chemistry of this process (McKenzie and O'Nions, 1991; Sparks and Cheadle, 1993). The approach adopted here is an "inverse" one, in which the temperatures and pressures of melt segregation are constrained directly from the geochemistry of the lavas.

In the case of the Greenland picrites and Gorgona komatiites shown in Fig. 7, the pressure of melt segregation can be inferred to have been similar to the pressure of melt initiation. Otherwise, the solidus character of these liquids would have been destroyed. Advanced equilibrium melting along the adiabat shown in Fig. 7 would have proceeded in the following way: [L + Ol + Opx + Cpx + Gt] → [L + Ol + Opx + Cpx] → [L + Ol + Opx]. Garnet would have been the first phase to be consumed, but this is inconsistent with the trace elements that show depletions in the HREE (Aitken and Echeverria, 1984; Holm et al., 1993), and with the systematics in Al_2O_3–CaO/Al_2O_3 (Fig. 4b). The degree of partial melting has been estimated to be <30% for an assumed average mantle peridotite source (Herzberg, 1992).

The most important observation in Fig. 7 is that the *T*–*P* conditions of melting and melt segregation for the Greenland picrites and Gorgona komatiites were 200°C higher than ambient mantle below ridges at 3–4 GPa. And since the pressures of melting of Hawaii are similar (Fig. 4a and b), it can be inferred that Hawaiian plume temperature is also ~200°C higher than ambient mantle. These compare with the 200–300°C excess temperatures that have been recommended for the present-day Hawaiian and Icelandic plumes (McKenzie, 1984; Yuen and Fleitout, 1985; Liu and Chase, 1989; Griffiths and Campbell, 1991; Watson and McKenzie, 1991).

If the Hawaiian plume is hotter than ambient mantle by 200°C, melting should be occurring at 100–125-km depth (3–4 GPa; Fig. 7), and this is consistent with slow S-wave velocities at 100–200 km (Zhang and Tanimoto, 1992). Komatiites with ~18% MgO should be forming below Hawaii (Fig. 1 and Albarède, 1992), similar to Gorgona Island. But volcanism on Hawaii is basaltic rather than komatiitic, and this points to the importance of olivine fractionation (Murata and Richter, 1966; O'Hara, 1968; Wright, 1972; Irvine, 1979; Albarède, 1992). A related question is therefore why plume volcanism is basaltic in some cases and komatiitic in others. Although this is well beyond the scope of this paper, it is worth noting that Hawaii differs from komatiite-yielding plumes in that clinopyroxene fractionation appears to have also been important (Feigenson et al., 1983; Fig. 4a, this work), and the occurrence of garnet exsolution in clinopyroxene xenocrysts (Beeson and Jackson, 1970) points to pressures of 2–3 GPa, corresponding to the lower portions of the lithosphere (Herzberg, 1978). The implication is that the strength or thickness of the lithosphere may be a factor in determining the eruptability of komatiites. Although the Earth could not have been much hotter during the Cretaceous (Fig. 8), there is an abundance of evidence that plume, ocean ridge and arc volcanism were much more widespread in the mid-Cretaceous than they are today, and this is correlated with other global phenomena such as a geomagnetic quite period, maximum sea-

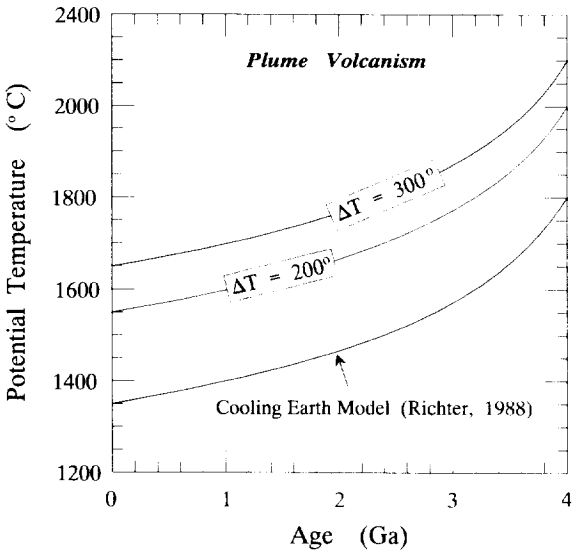

Fig. 8. Model of the variations in potential temperature below oceanic ridges through time, from Richter (1988). $\Delta T = 200°C$ and $\Delta T = 300°C$ represent excess plume temperatures.

level high stand and tropical climate extending into high latitudes (Larson, 1991; Storey et al., 1991; Sheridan, 1987). This unusual time in Earth history could have arisen from thermal instabilities that are characteristic of heat and mass transfer across endothermic phase transformations such as the 670-km discontinuity (Honda et al., 1993; Tackley et al., 1993; Steinbach and Yuen, 1994b), and this could have resulted in a lithosphere that was thinner or weaker in the Cretaceous compared to the present day.

For komatiites that are Archean in age, the temperatures of melting can be also be constrained from the solidus. However, in order to determine how these melting temperatures differed from ambient mantle at the time of formation, a thermal model for the Earth is needed. Following the suggestion of Nisbet et al. (1993), the cooling Earth model of Richter (1988) will be used here, and this is shown in Fig. 8.

Fig. 9 shows that most Munro-type komatiites with 2.7-Ga ages can be interpreted to have melted at ~5 GPa in a plume that was also ~200°C hotter than the ambient mantle of Richter (1988). This is based on the few Munro-type komatiites that plot near the solidus liquid line at 5–6 GPa (Fig. 5a) and on komatiites from the Newton Township (5–7 GPa; Fig. 5b). But a unique pressure cannot be determined for most Munro-type komatiites because they have the characteristics of liquids that segregated from a harzburgite source [L + Ol + Opx] (see above), and reference to Fig. 9 shows that orthopyroxene can coexist with olivine in the melting interval from 1 atm to ~9 GPa. Similarly, if melting occurred at much higher pressures than 9 GPa, then orthopyroxene would not have participated in the melting process, contrary to the geochemical evidence. Initial melting at 5–7 GPa is therefore realistic, and advanced melting during adiabatic decompression would have proceeded in the following way: [L + Ol + Opx + Cpx + Gt] → [L + Ol + Opx + Gt] → [L + Ol + Opx]. Liquids formed at each stage are represented in the Munro-type komatiite population, but most of them segregated from harzburgite [L + Ol + Opx] at a pressure that was probably < 5–7 GPa.

Although most 2.7-Ga komatiites can be understood as having formed in a plume that was 200°C hotter than the ambient mantle, those from the Boston Township seem to be an important exception (Xie et al., 1993).

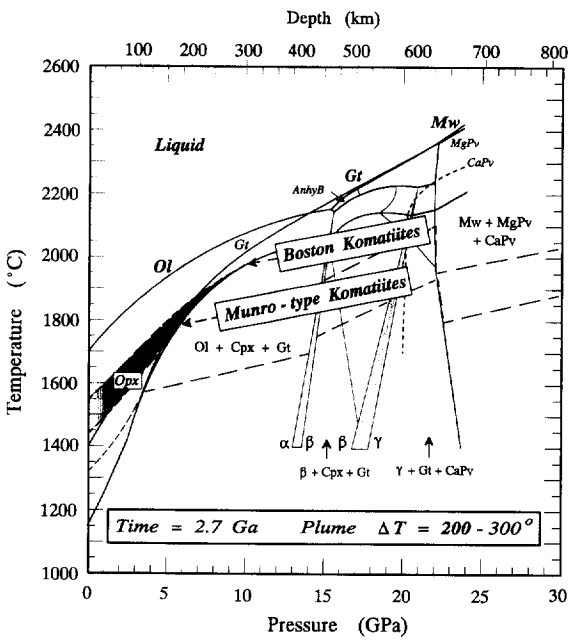

Fig. 9. Depths and temperatures of melting 2.7 Ga ago. *Lower dotted line* represents adiabat below ridges from Richter (1988; Fig. 8). Plumes that are 200° hotter can explain the geochemistry of most komatiites with 2.7-Ga ages. Komatiites from the Boston Township record 10–14 GPa (Fig. 5b), and require unusually hot plume temperatures (~300°C).

The Boston Township komatiites would have required a plume that was ~300°C hotter in order to generate the high-pressure signature that is indicated in their geochemistry (Fig. 5b). This is consistent with the interpretation of majorite garnet as a residual phase from the unusually strong depletions in Gd/Yb in addition to Hf and Zr with respect to neighbouring REE (Xie et al., 1993; McCuaig et al., 1994).

There is another possible way of explaining the Munro-type komatiites that have a strictly harzburgite geochemical signature. Since it is not possible to determine the *T–P* path that gives rise to an equilibrium assemblage, it is theoretically possible to explain the harzburgite geochemistry by crystallization as well as by melting. For example, it is possible that melting was deeper (e.g., 20 GPa) because it occurred in a plume that was ~400°C hotter than ambient 2.7-Ga mantle, and the harzburgite geochemistry was imprinted by crystallization and segregation at ~5 GPa. This is consistent with hot plume temperatures modelled by Steinbach and Yuen (1994a), and it may be a possible way of explaining the positive Hf and Zr anomalies in Munro komatiites reported by Xie et al. (1993). However, it would be difficult to explain the Newton Township komatiites (Cattell and Arndt, 1987) by this model, where both alumina-depleted and undepleted types occur together in space and time; the most simple explanation is that the alumina-depleted types were solidus melts formed at 5–7 GPa and at the periphery of a 200°C plume, and the alumina-undepleted types were higher degree melts that formed in the plume axis. I prefer a 200°C Munro plume to a 400°C one for its simplicity, but more work is clearly needed to resolve this important problem.

A plume that was 200°C hotter than Richter's (1988) ambient mantle at 3.5 Ga in the past would have melted at a pressure of 8 GPa (Fig. 10), and this could have generated some Barberton komatiites. But most Barberton komatiites record pressures of 9–10 GPa, and others record up to 14 GPa (Fig. 6). This indicates that an excess plume temperature of 200°C is somewhat too low, or the Archean mantle was hotter than Richter's (1988) estimate. The important observation is that a small increase in the plume temperature can make a large difference in depth of melting, and this is shown in Fig. 10; increasing the plume temperature from 200–300°C can increase the pressure of melt initiation from 8 to ~22 GPa. This occurs because the

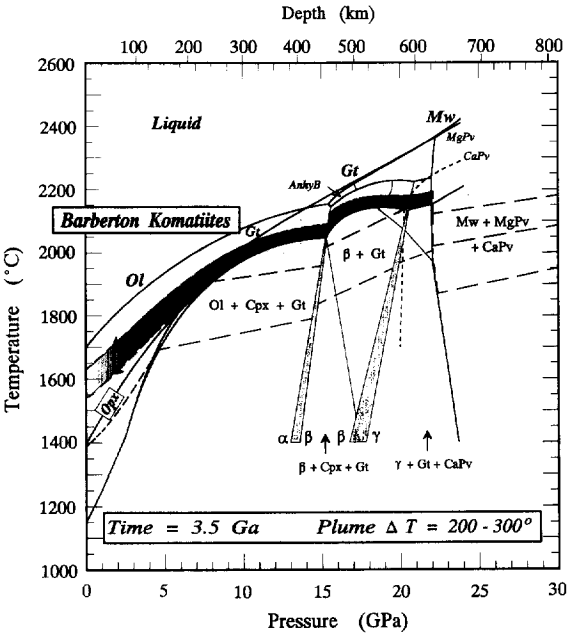

Fig. 10. Depths and temperatures of melting 3.5 Ga ago. *Lower dotted line* represents the adiabat below ridges, from Richter (1988; Fig. 8). Plumes that are 200°C hotter intersect the solidus at ~8 GPa, and plumes that are 300°C hotter can begin to melt at ~22 GPa. Barberton komatiites record pressures of 9–10 GPa, and possibly as high as 14 GPa (Fig. 6).

slope dT/dP of the solidus is very small at these pressures, and an ascending plume that encounters the transformation (Mg,Fe)O magnesiowüstite + $(Mg,Fe)SiO_3 \rightarrow \gamma(Mg,Fe)_2SiO_4$ must increase in temperature in order to maintain its adiabatic state (Ita and Stixrude, 1992; Steinbach and Yuen, 1994a). Widespread melting at 22 GPa should be expected for very hot plumes (Steinbach and Yuen, 1994a). Unfortunately, the compositions of these magmas are poorly known because of the paucity of experimental data. It is most likely, however, that they are substantially different from the Barberton komatiites, which have geochemical properties of liquids in the 9–14-GPa range (Fig. 6). Sparks and Cheadle (1993) have suggested that melting may have occurred at 22 GPa, but the compositions of the erupted Barberton komatiites are actually high-and low-pressure magmas that became mixed in the plume. It is possible, therefore, that Barberton komatiites that record a 14-GPa signature in their CaO/Al_2O_3 are actually mixtures of magmas that formed in the 10–22-GPa range.

Evidence for an early Archean period of very deep melting is also contained in the lithosphere peridotites from the Kaapvaal craton that are contained in kimberlite. These have a major-element geochemistry that differs from typical mantle peridotite and its pyrolite analogue (Boyd, 1989; Herzberg, 1993a), and they have been interpreted as harzburgite cumulates (Herzberg, 1993a) that formed from a plume that experienced melting in the 50–80% range (Herzberg, 1993a). This degree of melting is higher than that which was experienced by any other type of komatiite, and in order for such an extensive amount of melt to have formed, melting itself probably commenced at pressures in excess of 20 GPa (Miller et al., 1991), corresponding to the top of the lower mantle. This could have been accomplished by a plume that was 300–400°C hotter than Richter's ambient mantle at 3.3 ± 0.3 Ga ago, about the time that these rocks formed (Pearson et al., 1995). The first continental lithosphere and crust at ~3.3 Ga may therefore have formed from a gigantic plume within which melting was deeper and more extensive than at any other time in Earth history (Herzberg, 1993a; Pearson et al., 1995).

7. Discussion

Secular variations in the geochemistry of komatiites have been recognized for some time (Jahn et al., 1982; Gruau et al., 1990), and they can be interpreted as arising from secular variations in the depth of melting and melt segregation (Fig. 6). Older komatiites experienced deeper melting, and the higher pressures stabilize garnet relative to olivine and pyroxenes, resulting in komatiites with lower Al_2O_3, and higher CaO/Al_2O_3 and Gd/Yb. Although the relationship between depth and temperature of melting can be easily constrained with the phase diagram, more difficult to understand is the relationship between the depth of melting and the thermal state of the Earth at the time.

If komatiites formed along ridges as suggested by Takahashi (1990), the secular variations in temperature and pressure of melting recorded in their geochemistry would be a straightforward measure of the thermal state of the Earth through time. But the high temperatures create difficulties with this model (Nisbet et al., 1993), and it is more likely that they formed in plumes instead (Jarvis and Campbell, 1983; Campbell et al., 1989; Herzberg, 1992). It then becomes important to determine the relationship between the thermal properties of plumes and the thermal state of the Earth during the time of their formation.

The cooling Earth model of Richter (1988) predicts an Earth that was hotter by 180° and 300°C during the Archean 2.7 and 3.5 Ga ago, respectively (Fig. 8). Most picrites and komatiites that range in age from 60 to 3500 Ma can be interpreted to record conditions of melting that were hotter than Richter's (1988) ambient mantle by 200°C. The results presented here are in excellent agreement with the 200–300°C excess temperatures calculated by Nisbet et al. (1993) and Abbott et al. (1994), based on the MgO content of komatiites. Richter's (1988) model therefore suggests that the 200°C excess temperature may be a characteristic of plumes of all ages, and secular variations observed in the geochemistry of komatiites were an outcome of a hotter Earth rather than hotter plumes. The geochemistry of komatiites would then be the most direct way of measuring the thermal state of the Earth in the past.

But there are theoretical lines of evidence that indicate the existence of hotter plumes with excess temperatures in the 300°–400°C range (Sparks and Cheadle, 1993; Steinbach and Yuen, 1994a). The phase diagram for mantle peridotite would require very deep melting, extending into the transition zone and top of the lower mantle for a suitably hot Earth (Fig. 10). Although there is a paucity of geological evidence for deep melting in hot plumes, it can be found in the 2.7-Ga komatiites from the Boston Township in Ontario (Xie et al., 1993; McCuaig et al., 1994) and the 3.3-Ga peridotite xenoliths from the Kaapvaal craton (Herzberg, 1993a; Pearson et al., 1995). Discriminating between 200° and 400°C plumes is therefore an important challenge because of the implications concerning depth of melting and mass transport throughout the Earth.

A promising new way to test the hot 400°C plume and deep melting possibility is the one taken by Xie et al. (1993) and McCuaig et al. (1994) wherein trace-element partitioning studies (e.g., Kato et al., 1988; Ohtani et al., 1989) have been combined with a determination of trace-element abundances in komatiites to evaluate the prospects of deep mantle phases. A definitive signature of either perovskite or magnesiowüstite would be a convincing test of deep melting in superhot plumes. It is therefore very important that there be a

resolution to analytical differences reported on similar komatiites from different laboratories (Jochum et al., 1991; Xie et al., 1993).

Acknowledgements

This research was partially supported by a grant from the National Science Foundation (EAR 94-06976). Mike Cheadle, Bob Luth, Rob Kerrich and Dave Yuen are thanked for critical reviews and stimulating discussions. Special thanks go to Nick Arndt for discussions and the opportunity to attend the workshop in St. Malo. This is Mineral Physics Institute Publication No. 130 at the Department of Earth and Space Sciences, SUNY, Stony Brook.

Appendix A

Mantle peridotite exhibits a range of possible values for CaO/Al_2O_3 and Al_2O_3, and a compilation of 542 spinel lherzolite analyses (Herzberg, 1993a) is shown in Fig. 11. Some of the scatter in CaO/Al_2O_3 arises from analytical error stemming from refractory peridotite samples with inherently low concentrations of CaO and Al_2O_3. However, some high values of CaO/Al_2O_3 are correlated with FeO/MgO, and are likely to represent a komatiite component (see also Herzberg, 1993a).

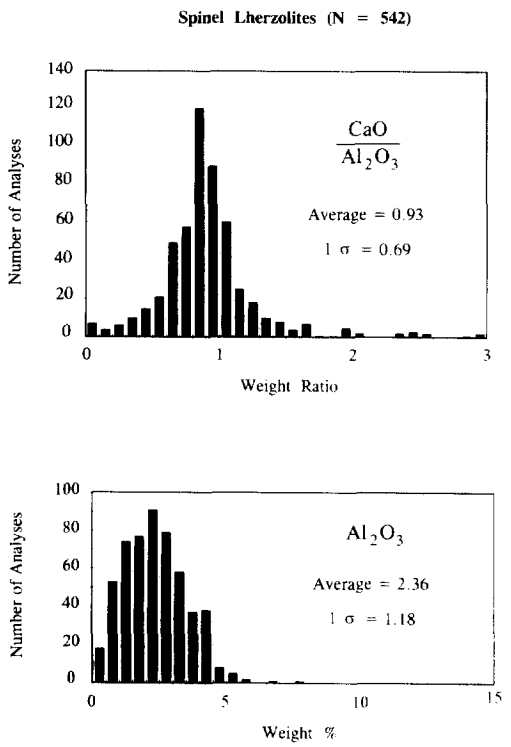

Fig. 11. The content of Al_2O_3 and CaO/Al_2O_3 in mantle peridotite (Herzberg, 1993a).

References

Abbott, D., Burgess, L. and Longhi, J., 1994. An empirical thermal history of the Earth's upper mantle. J. Geophys. Res., 99: 13,835–13,850.

Aitken, B.G. and Echeverria, L.M., 1984. Petrology and geochemistry of komatiites and tholeiites from Gorgona Island, Colombia. Contrib. Mineral. Petrol., 86: 94–105.

Albarède, F., 1992. How deep do common basaltic magmas form and differentiate? J. Geophys. Res., 97: 10,997–11,009.

Arndt, N.T., 1986. Komatiites: a dirty window to the Archean mantle. Terra Cognita, 6: 59–66.

Arndt, N.T. and Lesher, C.M., 1992. Fractionation of REEs by olivine and the origin of Kambalda komatiites, Western Australia. Geochim. Cosmochim. Acta, 56: 4191–4204.

Arndt, N.T. and Nisbet, E.G., 1982. What is a komatiite? In: N.T. Arndt and E.G. Nisbet (Editors), Komatiites. George Allen & Unwin, London, pp. 19–27.

Arndt, N.T., Naldrett, A.J. and Pyke, D.R., 1977. Komatiitic and iron-rich tholeiitic lavas of Munro Township, Northeast Ontario, J. Petrol., 18: 319–369.

Arth, J.G., Arndt, N.T. and Naldrett, A.J., 1977. Genesis of Archean komatiites from Munro Township, Ontario: trace element evidence. Geology, 5: 590–594.

Baker, M.B. and Stolper, E.M., 1994. Determining the composition of high-pressure mantle melts using diamond aggregates. Geochim. Cosmochim. Acta, 58: 2811–2827.

Beattie, P., 1993. Olivine–melt and orthopyroxene–melt equilibria. Contrib. Mineral. Petrol., 115: 103–111.

Beeson, M.H. and Jackson, E.D., 1970. Origin of the garnet pyroxenite xenoliths at Salt Lake Crater, Oahu. Mineral. Soc. Am., Spec. Pap., 3: 95–112.

Bertka, C. and Holloway, J.F., 1988. Martian mantle primary melts: an experimental study of iron-rich garnet lherzolite minimum melt compositions. Proc. 18th Lunar Planet. Sci. Conf., pp. 723–739.

Boyd, F.R., 1989. Compositional distinction between oceanic and cratonic lithosphere. Earth Planet. Sci. Lett., 96: 15–26.

Campbell, I.H., Griffiths, R.W. and Hill, R.I., 1989. Melting in an Archaean mantle plume: heads it's basalts, tails it's komatiites. Nature (London), 339: 697–699.

Cattell, A. and Arndt, N., 1987. Low-and high-alumina komatiites from a Late Archaean sequence, Newton Township, Ontario. Contrib. Mineral. Petrol., 97: 218–227.

Clague, D.A., Weber, W.S. and Dixon, J.E., 1991. Picritic glasses from Hawaii. Nature (London), 353: 553–556.

Davis, B.T.C. and Schairer, J.F., 1965. Melting relations in the join diopside–forsterite–pyrope at 40 kilobars and at one atmosphere. Carnegie Inst., Washington, Yearbk., 64: 123–126.

Duncan, R.A. and Hargraves, R.B., 1984. Plate tectonic evolution of the Caribbean region in the mantle reference frame. In: W.E. Bonini, R.B. Hargraves and R. Shagam (Editors), The Caribbean–South American Plate Boundary and Regional Tectonics. Geol. Soc. Am., Mem., 162: 81–93.

Echeverria, L.M., 1982. Komatiites from Gorgona Island, Colombia. In: N.T. Arndt, N.T. and E.G. Nisbet (Editors), Komatiites. George Allen & Unwin, London, pp. 199–209.

Falloon, T.J. and Green, D.H., 1988. Anhydrous partial melting of peridotite from 8 to 35 kb and the petrogenesis of MORB. J. Petrol., Spec. Lithosphere Iss., pp. 379–414.

Feigenson, M.D., Hofmann, A.W. and Spera, F.J., 1983. Case studies on the origin of basalt, II. The transition from tholeiitic to alkalic volcanism on Kohala volcano, Hawaii. Contrib. Mineral. Petrol., 84: 390–405.

Fitton, G. and Saunders, A., 1994. Magma sources and plumbing during continental breakup. Workshop on Mafic Magmatism Through Time, St. Malo, May 1994.

Fujii, T., Tachikara, M. and Kurita, K., 1989. Melting experiments in the system $CaO–MgO–Al_2O_3–SiO_2$ to 8 GPa: Constraints to the origin of komatiites. Eos (Trans. Am. Geophys. Union), 70: 483 (abstract).

Fyfe, W.S., 1978. The evolution of the Earth's crust: modern plate tectonics to ancient hot spot tectonics? Chem. Geol., 23: 89–114.

Griffiths, R.W. and Campbell, I.H., 1991. On the dynamics of long-lived plume conduits in the convecting mantle. Earth Planet. Sci. Lett., 103: 214–227.

Gruau, G., Jahn, B.M., Glikson, A.Y., Davy, R., Hickman, A.H. and Chauvel, C., 1987. Age of the Archean Talga–Talga subgroup, Pilbara block, Western Australia, and early evolution of the mantle: New Sm–Nd isotopic evidence. Earth Planet. Sci. Lett., 85: 105–116.

Gruau, G., Chauvel, C., Arndt, N.T. and Cornichet, J., 1990. Aluminum depletion in komatiites and garnet fractionation in the early Archean mantle: Hafnium isotopic constraints. Geochim. Cosmochim. Acta, 54: 3095–3101.

Hanson, G.N. and Langmuir, C.H., 1978. Modelling of major elements in mantle–melt systems using trace element approaches. Geochim. Cosmochim. Acta, 42: 725–741.

Herzberg, C.T., 1978. The bearing of phase equilibria in simple and complex systems on the origin and evolution of some well-documented garnet-websterites. Contrib. Mineral. Petrol., 66: 375–382.

Herzberg, C., 1983. Solidus and liquidus temperatures and mineralogies for anhydrous garnet-lherzolite to 15 GPa. Phys. Earth Planet. Inter., 32: 193–202.

Herzberg, C., 1992. Depth and degree of melting of komatiites. J. Geophys. Res., 97: 4521–4540.

Herzberg, C.T., 1993a. Lithosphere peridotites of the Kaapvaal craton. Earth Planet. Sci. Lett., 120: 13–29.

Herzberg, C.T., 1993b. Magmatism in plumes and hot spots. Eos (Trans. Am. Geophys. Union), 74: 81 (abstract).

Herzberg, C.T. and O'Hara, M.J., 1985. Origin of mantle peridotite and komatiite by partial melting. Geophys. Res. Lett., 12: 541–544.

Herzberg, C.T. and Zhang, J., 1995. Melting experiments on peridotite to 22.5 GPa: phase chemistry. Trans. Am. Geophys. Union, 76: 5297.

Herzberg, C.T., Gasparik, T. and Sawamoto, H., 1990. Origin of mantle peridotite: constraints from melting experiments to 16.5 GPa. J. Geophys. Res., 95: 15,779–15,803.

Hirose, K. and Kushiro, I., 1993. Partial melting of dry peridotites at high pressures: Determination of compositions of melts segregated from peridotite using aggregates of diamond. Earth Planet. Sci. Lett., 114: 477–489.

Hirschmann, M.M. and Ghiorso, M.S., 1994. Activities of nickel, cobalt, and manganese silicates in magmatic liquids and applications to olivine/liquid and to silicate/metal partitioning. Geochim. Cosmochim. Acta, 58: 4109–4126.

Holm, P.M., Gill, R.C.O., Pedersen, A.K., Larsen, J.G., Hald, N., Nielsen, T.F.D. and Thirlwall, M.F., 1993. The Tertiary picrites of West Greenland: contributions from "Icelandic" and other sources. Earth Planet. Sci. Lett., 115: 227–244.

Honda, S., Yuen, D., Balachandar, S. and Reuteler, D., 1993. Three-dimensional instabilities of mantle convection with multiple phase transitions. Science, 259: 1308–1311.

Irvine, T.N., 1979. Rocks whose composition is determined by crystal accumulation and sorting. In: H.S. Yoder (Editor), The Evolution of the Igneous Rocks. Princeton University Press, Princeton, N.J., pp. 245–306.

Ita, J. and Stixrude, L., 1992. Petrology, elasticity, and composition of the mantle transition zone. J. Geophys. Res., 97: 6849–6866.

Jahn, B.-M., Vidal, P. and Tilton, G.R., 1980. Archean mantle heterogeneity: evidence from chemical and isotopic abundances in Archean igneous rocks. Philos. Trans. R. Soc. London, Ser. A, 297: 353–364.

Jahn, B.-M., Gruau, G. and Glikson, A.Y., 1982, Komatiites of the Onverwacht Group, S. Africa: REE geochemistry, Sm/Nd age and mantle evolution. Contrib. Mineral. Petrol., 80: 25–40.

Jarvis, G.T. and Campbell, I.H., 1983. Archean komatiites and geotherms: solution to an apparent contradiction. Geophys. Res. Lett., 10: 1133–1136.

Jochum, K.P., Arndt, N.T. and Hofmann, A.W., 1991. Nb–Th–La in komatiites and basalts: constraints on komatiite petrogenesis and mantle evolution. Earth Planet. Sci. Lett., 107: 272–289.

Kato, T., Ringwood, A.E. and Irifune, T., 1988. Experimental determination of element partitioning between silicate perovskites, garnets and liquids: constraints on early differentiation of the mantle. Earth Planet. Sci. Lett., 89: 123–145.

Kerr, A. and Marriner, G., 1994. Columbian/Caribbean plateau basalts. Workshop on Mafic Magmatism Through Time, St. Malo, May 1994.

Langmuir, C.H., Klein, E.M. and Plank, T., 1992. Petrological systematics of mid-ocean ridge basalts: Constraints on melt generation beneath ocean ridges. In: J. Phipps Morgan, D.K. Blackman and J. Sinton (Editors), Mantle Flow and Melt Generation at Mid-Ocean Ridges. Am. Geophys. Union, 71: 183–280.

Larson, R.L., 1991. Latest pulse of the Earth: evidence for mid-Cretaceous superplume. Geology, 19: 547–550.

Lécuyer, C., Gruau, G., Anhaeusser, C.R. and Fourcade, S., 1994. The origin of fluids and the effects of metamorphism on the primary chemical compositions of Barberton komatiites: New

evidence from geochemical (REE) and isotopic (Nd, O, H, $^{39}Ar/^{40}Ar$) data. Geochim. Cosmochim. Acta, 58: 969–984.

Liu, M. and Chase, C.G., 1989. Evolution of midplate hot spot swells: numerical solutions. J. Geophys. Res., 94: 5571–5584.

McCuaig, T.C., Kerrich, R. and Xie, Q., 1994. Phosphorus and high field strength element anomalies in Archean high-magnesian magmas as possible indicators of source mineralogy and depth. Earth Planet. Sci. Lett., 124: 221–239.

McKenzie, D.P., 1984. The generation and compaction of partial molten rock. J. Petrol., 25: 713–765.

McKenzie, D. and Bickle, M.J., 1988. The volume and composition of melt generated by extension of the lithosphere. J. Petrol., 29: 625–679.

McKenzie, D. and O'Nions, R.K., 1991. Partial melt distributions from inversion of rare earth element concentrations. J. Petrol., 32: 1021–1091.

Miller, G.H., Stolper, E.M. and Ahrens, T.J., 1991. The equation of state of a molten komatiite, 2. Application to komatiite petrogenesis and the Hadean mantle. J. Geophys. Res., 96: 11,849–11,864.

Murata, K.J. and Richter, D.H., 1966. Chemistry of the lavas of the 1959–1960 eruption of Kilauea volcano, Hawaii. U.S. Geol. Surv., Prof. Pap., 537-A: 1–26.

Nesbitt, R.W. and Sun, S.-s., 1976. Geochemistry of Archaean spinifex-textured peridotites and magnesian and low-magnesian tholeiites. Earth Planet. Sci. Lett., 31: 433–453.

Nesbitt, R.W., Sun, S.-s. and Purvis, A.C., 1979. Komatiites: geochemistry and genesis. Can. Mineral., 17: 165–186.

Nisbet, E.G., Arndt, N.T., Bickle, M.J., Camerson, W.E., Chavel, C., Cheadle, M., Hegner, E., Kyser, T.K., Martin, A., Renner, R. and Roedder, E., 1987. Uniquely fresh 2.7 Ga komatiites from the Belingwe greenstone belt, Zimbabwe. Geology, 15: 1147–1150.

Nisbet, E.G., Cheadle, M.J., Arndt, N.T. and Bickle, M.J., 1993. Constraining the potential temperature of the Archaean mantle: A review of the evidence from komatiites. Lithos, 30: 291–307.

O'Hara, M.J., 1968. The bearing of phase equilibria studies in synthetic and natural systems on the origin and evolution of basic and ultrabasic rocks. Earth-Sci. Rev., 4: 69–133.

O'Hara, M.J., Saunders, M.J. and Mercy, E.P.L., 1975. Garnet-peridotite, primary ultrabasic magma and eclogites; interpretation of upper mantle processes in kimberlite. Phys. Chem. Earth, 9: 571–604.

Ohtani, E., Kawabe, I., Moriyama, J. and Nagata, Y., 1989. Partitioning of elements between majorite garnet and melt and implications for petrogenesis of komatiite. Contrib. Mineral. Petrol., 103: 263–269.

Pearson, D.G., Carlson, R.W., Shirey, S.B., Boyd, F.R. and Nixon, P.H., 1995. The stabilization of Arhaean lithospheric mantle: a Re–Os isotope study of peridotite xenoliths from the Kaapvaal and Siberian cratons. Earth Planet. Sci. Lett., 134: 341–357.

Presnall, D.C., Dixon, J.R., O'Donnell, T.H. and Dixon, S.A., 1979. Generation of mid-ocean ridge tholeiites. J. Petrol., 20: 3–35.

Richter, F.M., 1988. A major change in the thermal state of the Earth at the Archaean–Proterozoic Boundary: Consequences for the nature and preservation of continental lithosphere. J. Petrol., Spec. Lithosphere Iss., 39–52.

Salters, V.J.M. and Hart, S.R., 1989. The hafnium paradox and the role of garnet in the source of mid-ocean-ridge basalts. Nature (London), 342: 420–422.

Sheridan, R.E., 1987. Pulsation tectonics as the control of long-term stratigraphic cycles. Paleooceanography, 2: 97–118.

Shimazaki, T. and Takahashi, E., 1993. High-pressure melting of a peridotite KLB-1: on the early melting history of the Earth. Eos (Trans. Am. Geophys. Union), 74: 655 (abstract).

Smith, H.S. and Erlank, A.J., 1982. Geochemistry and petrogenesis of komatiites from the Barberton greenstone belt, South Africa. In: N.T. Arndt and E.G. Nisbet (Editors), Komatiites. George Allen & Unwin, London, pp. 347–397.

Sparks, D.W. and Cheadle, M.J., 1993. Thermodynamic modelling of melting in mantle plumes: komatiites, the ultimate test. Eos (Trans. Am. Geophys. Union), 74: 594 (abstract).

Steinbach, V. and Yuen, D.A., 1994a. Melting instabilities in the transition zone. Earth Planet. Sci. Lett., 127: 67–75.

Steinbach, V. and Yuen, D.A., 1994b. Effects of depth-dependent properties on the thermal anomalies produced in flush instabilities from phase transitions. Phys. Earth Planet. Inter., 86: 165–183.

Stone, W.E., Jensen, L.S. and Church, W.R., 1987. Petrography and geochemistry of an unusual Fe-rich basaltic komatiite from Boston Township, northeastern Ontario. Can. J. Earth Sci., 24: 2537–2550.

Storey, M., Mahoney, J.J., Kroenke, L.W. and Saunders, A.D., 1991. Are oceanic plateaus sites of komatiite formation? Geology, 19: 376–379.

Stosch, H.-G. and Seck, H.A., 1980. Geochemistry and mineralogy of two spinel peridotite suites from Dreiser Weiher, West Germany. Geochim. Cosmochim. Acta, 44: 457–470.

Sun, S.-s. and Nesbitt, R.W., 1978. Petrogenesis of Archaean ultrabasic and basic volcanics: evidence from rare earth elements. Contrib. Mineral. Petrol., 65: 301–325.

Tackley, P.J., Stevenson, D.J., Glatzmaier, G.A. and Schubert, G., 1993. Effects of an endothermic phase transition at 670 km depth in a spherical model of convection in the Earth's mantle. Nature (London), 361: 699–704.

Takahashi, E., 1986. Melting of a dry peridotite KLB-1 up to 14 GPa: implications on the origin of peridotitic upper mantle. J. Geophys. Res., 91: 9367–9382.

Takahashi, E., 1990. Speculations on the Archean mantle: missing link between komatiite and depleted garnet peridotite. J. Geophys. Res., 95: 15,941–15,954.

Tronnes, R.G., Canil, D. and Wei, K., 1992. Element partitioning between silicate and coexisting melts at pressures of 1–27 GPa, and implications for mantle evolution. Earth Planet. Sci. Lett., 111: 241–255.

Watson, S. and McKenzie, D., 1991. Melt generation by plumes: a study of Hawaiian volcanism. J. Petrol., 32: 501–537.

Wei, K., Tronnes, R.G. and Scarfe, C.M., 1990. Phase relations of aluminum-undepleted and aluminum-depleted komatiites at pressures of 4–12 GPa. J. Geophys. Res., 95: 15,817–15,828.

Wright, T.L., 1972. Chemistry of Kilauea and Mauna Loa lava in space and time. U.S. Geol. Surv., Prof. Pap., 735: 1–39.

Xie, Q., Kerrich, R. and Fan, J., 1993. HFSE/REE fractionations recorded in three komatiite–basalt sequences, Archean Abitibi

greenstone belt: Implications for multiple plume sources and depths. Geochim. Cosmochim. Acta, 57: 4111–4118.

Yuen, D. and Fleitout, L., 1985. Thinning of the lithosphere by small-scale convective destabilization. Nature (London), 313: 125–127.

Yurimoto, H. and Ohtani, E., 1992. Element partitioning between majorite and liquid: a secondary ion mass spectrometric study. Geophys. Res. Lett., 19: 17–20.

Zhang, J. and Herzberg, C., 1994a. Melting experiments on anhydrous peridotite KLB-1 from 5.0 to 22.5 GPa. J. Geophys. Res., 99: 17,729–17,742.

Zhang, J. and Herzberg, C., 1994b. Melting of pyrope, $Mg_3Al_2Si_3O_{12}$, at 7–16 GPa. Am. Mineral., 79: 497–503.

Zhang, Y.-S. and Tanimoto, T., 1992. Ridges, hotspots and their interaction as observed in seismic velocity maps. Nature (London), 355: 45–49.